Flight Performance Maneuver Planning for NASA's X-57 "Maxwell" Flight Demonstrator – Part 2: Power-On Effects

Nicholas K. Borer[1]
NASA Langley Research Center, Hampton, Virginia, 23681, USA

James R. Reynolds[2] and Ryan D. Wallace[3]
NASA Armstrong Flight Research Center, Edwards, California, 93523, USA

Distributed Electric Propulsion technology as envisioned for NASA's X-57 "Maxwell" flight demonstrator concept was designed to increase high-speed cruise efficiency compared to a combustion-powered general aviation baseline. A portion of this increased efficiency was due to beneficial aero-propulsive interaction inherent to the distributed propulsion architecture. The measure of the increase in efficiency between a conventional and distributed propulsion wing was to be determined by comparing flight test data from the electrically powered, conventional wing X-57 Mod II configuration to data obtained from the electrically powered, distributed propulsion wing X-57 Mod III/IV configuration. Flight test maneuvers that accommodate errors in instrumentation and the flight test environment were previously developed to establish the power-off drag characteristics for all X-57 configurations. In this paper, test points and maneuvers are evaluated to establish the installed and gross thrust that build upon the power-off drag estimates. Analysis of the proposed power-on maneuvers shows that the selected test points and measurement techniques could generate installed thrust estimates within 3-7% (at the 50% confidence level) of the actual values if each maneuver is conducted over a time period of 40 seconds.

I. Nomenclature

C_D	coefficient of drag	q	freestream dynamic pressure
C_L	coefficient of lift	Q	motor or propeller shaft torque
C_P	power coefficient	S	reference area
C_T	thrust coefficient	T	thrust
D	power-off drag force	V	true airspeed, relative to aircraft wind axes
D_p	propeller diameter	W	aircraft weight
$F_{x_{wind}}$	x-axis of the wind frame	α	angle of attack
$F_{z_{wind}}$	z-axis of the wind frame	γ	flight path angle
g_0	acceleration due to gravity	Δh	change in altitude
$\dot{h}$	rate of change of altitude (also rate of climb)	Δt	elapsed time
J	propeller advance ratio	η_p	propeller efficiency
K_i	coefficients in drag model (i = 0, 1, or 2)	θ	angle of pitch
L	lift force	ρ	air density
m	aircraft mass	σ	standard deviation of a normal distribution
n	propeller speed		

[1] X-57 Performance and Sizing Team Lead, Aeronautics Systems Analysis Branch, AIAA Associate Fellow.
[2] X-57 Controls Team Lead, Dynamics and Controls Branch, Nonmember.
[3] X-57 Controls Team, Dynamics and Controls Branch, AIAA Senior Member.

II. Introduction

The X-57 "Maxwell" was a NASA flight demonstrator concept* for Distributed Electric Propulsion (DEP) technology. This technology resulted from the confluence of *distributed propulsion* (the integration of propulsive devices strategically placed about the airframe to yield aero-propulsive benefits) and *electrified propulsion* (the use of electric machines to drive propulsive devices). DEP technology was expected to yield a substantial reduction in onboard energy consumption for the X-57 in high-speed cruise flight [1], compared to the donor Tecnam P2006T [2], a conventionally fueled, combustion-powered aircraft that has a fuselage, empennage, and landing gear in common with the X-57.

The energy consumption reduction target associated with DEP on the X-57 was apportioned between the use of *electrified propulsion* (compared to the gasoline engine on the P2006T) and the use of *distributed propulsion* (the aero-propulsive benefits of the X-57 distributed propulsion wing compared to the P2006T wing). These were referred to in the top-level X-57 project's objectives as OBJ-1 and OBJ-2, respectively. The minimum success criteria associated with these objectives were as follows:

- X-57 OBJ-1: Consume less than 33% of the energy of a baseline General Aviation (GA) aircraft at high-speed cruise.
- X-57 OBJ-2: Consume less than 83% of the energy of an electric GA aircraft with a conventional wing at high-speed cruise.

An appropriate "high-speed cruise" target was explored in Ref. [1] and was also defined in the X-57 Performance and Sizing requirements as steady, level flight at 150 knots true airspeed (KTAS) at 8,000 ft above Mean Sea Level (MSL) in the 1976 U.S. Standard Atmosphere [3].

The combined effects of OBJ-1 and OBJ-2 results in an aircraft that consumes approximately $0.33 \times 0.83 = 27\%$ of the energy of a gasoline-fueled, conventionally configured baseline aircraft. However, these were the project objectives from which all system requirements were derived and therefore represented the minimum achievable standard for project success. The project *goal* was a combined 20% energy consumption metric compared to the baseline GA aircraft ("fivefold reduction in energy consumption" per Ref. [1]). Estimates provided at the X-57 critical design review showed that the distributed propulsion wing could result in an energy consumption that was 65% of an electric aircraft with a conventional wing, exceeding the requirement in OBJ-2 [4] in an attempt to push X-57's energy consumption closer towards the goal, rather than simply meeting the objective.

If the cruise propulsion system had negligible effects on the aerodynamics of the conventionally configured electric aircraft, X-57 OBJ-1 could largely be inferred through ground tests. That is, if the power requirements at the high-speed cruise point were known for either the combustion-powered or electric variant, then a ground test could be used to measure the efficiency of the electric powertrain at this power setting† versus the efficiency of the combustion engine (presuming any altitude effects on power setting and efficiency were duplicated in the ground test environment). The X-57 project planned to use this approach to determine compliance with OBJ-1. However, determination of the aero-propulsive benefit of X-57's distributed propulsion architecture required operation in flight or powered wind tunnel environments to ensure that the interacting aero-propulsive effects were properly captured.

A. X-57 Spiral Development Approach

Demonstration of new technologies can be a challenging endeavor and requires a systematic approach to manage risk. The X-57 project planned a spiral development approach, which involved several different configuration modifications, or Mods, as shown in Fig. 1. These Mods were to serve as interim demonstrations to reduce risk by testing different aspects of new hardware, software, and/or flight phenomena sequentially, rather than all at once.

Mod I flights, completed in 2015, established the baseline, gasoline-powered aircraft performance. The Mod II configuration replaced the two gasoline engines on the stock Tecnam P2006T with electric motors and installed the X-57 high-voltage energy storage system in the aft cabin and cargo area. This Mod was intended to verify the flight readiness of the electric propulsion system. Mod III would have replaced the large P2006T wing with a much smaller wing suitable for DEP and moved the cruise motors tested on Mod II out to the wingtips. This configuration was intended to test high-speed cruise efficiency, including aerodynamic and aero-propulsive benefits, of the modified DEP wing. Mod IV would have used the same wing design as Mod III with the addition of 12 high-lift motors to compare the low-speed performance of the DEP-enabled aircraft to the original aircraft.

---

* NASA ended the X-57 project prior to flight of any of the electrified configurations, so we present this information to assist other related endeavors.

† We recognize that such a test would not resolve differences in power setting for a given flight condition due to installation or cooling drag differences between the electric and combustion configuration.

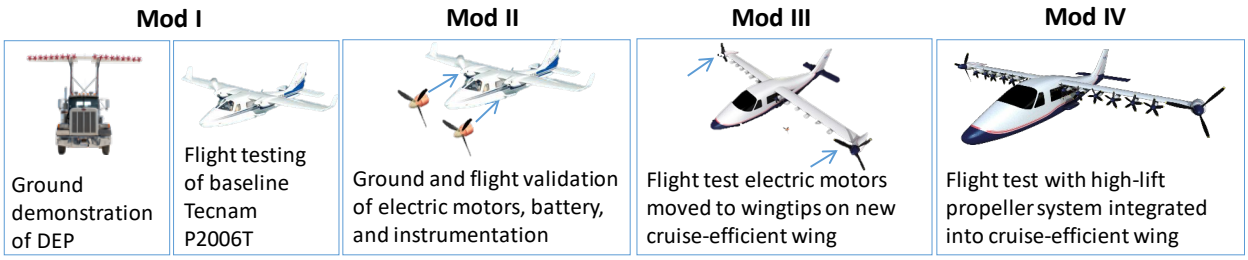

Fig. 1 X-57 development through multiple "Mods" [1].

The performance of the aircraft per the criteria of X-57 OBJ-2 was to be measured by comparing the flight data from X-57 Mod II with flight data from X-57 Mod III. The X-57 instrumentation system was designed to capture detailed information on the current and voltage associated with the traction electrical bus, which could determine the power consumption at any given setting. However, it is generally impossible to perfectly match test conditions between flights, so performance models of the X-57 Mod II and Mod III configurations were planned to help normalize conditions for later comparison. This is standard practice for aircraft performance comparison; it is nearly impossible to directly compare flight data between two different flight tests without a tightly controlled environment (e.g., in a wind tunnel). These performance models were planned to be built from two types of maneuvers: power-off glides and power-on climbs and level flight. The methods planned for data reduction of the power-off glides were described in a previous paper [5], and the methods used for power-on maneuvers are the subject of this paper. The methods used to establish power-on data included analysis of different in-flight test points and measurement tolerances.

III. Power-On Performance Estimation

The purpose of the power-on tests was to determine the installed thrust of the X-57 propulsion system. The *installed thrust* is defined as the thrust force generated by the X-57 propulsion units after accounting for interactions of the propulsor with the airframe (as compared to the theoretical thrust force from the propulsor in isolation) [6]. For propeller-driven aircraft (like the X-57), these interactions include cooling drag,[‡] scrubbing,[§] and blockage,[**] all of which tend to reduce the amount of thrust generated by a propeller as compared to the same isolated propeller (which is known as *gross thrust*). Additionally, the axial and rotating components of the propeller slipstream can modify the lift distribution of the wing, which can lead to changes in the lift-induced drag. This latter effect was of particular importance to the X-57 project. In the Mod I and II configurations, the propellers mounted on the inboard section of the wing would yield changes to the lift distribution that tend to increase lift-induced drag [7] compared with the Mod III and IV configurations where the wingtip-mounted cruise propellers were designed to reduce the lift-induced drag [8]. The change in installation effects was an important discriminator and formed the rationale for power-off glide and power-on test points.

A. Installed Thrust Calculation

The installed thrust was estimated using the power-off drag estimates developed in the previous paper [5]. The salient forces acting on the aircraft in powered flight are shown in Fig. 2, as are other pertinent parameters. Here, L is the lift force perpendicular to the velocity vector, D is the drag force acting opposite to the velocity vector, T is the thrust force, and mg_0 is the weight, W, of the aircraft based on the mass, m, and the acceleration due to gravity, g_0. Figure 2 also depicts the true airspeed, V, acting along the aircraft velocity vector, the pitch angle relative to the horizon, θ, the angle of attack, α, and the flight path angle, γ. In this case, the thrust vector is assumed to act along the body x-axis, though this may not be the case for all aircraft.

[‡] Cooling drag refers to momentum loss associated with cooling temperature-critical components of the propulsion system and can include cooling air intake, internal flow losses through ducting and radiators, and cooling air exhaust.
[§] Scrubbing refers to increased parasite drag associated with the higher-velocity air in the slipstream of a propeller as compared to the freestream.
[**] Blockage refers to obstructions upstream (such as propeller spinners) or downstream (such as engine nacelles) that modify the incoming flow into the propeller or that interact with the flow of the propeller slipstream, both of which impact the momentum transfer associated with propeller forces.

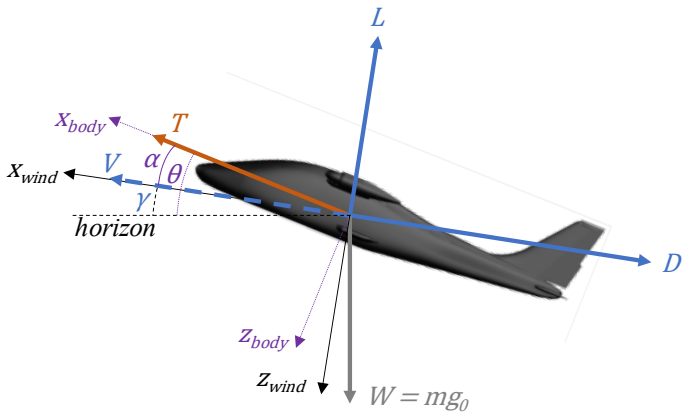

Fig. 2 Aircraft orientation and forces in wind and body axes.

The balance of these forces can be used to estimate the rate of change of altitude of the aircraft ("rate of climb"). Summing the forces along the wind x-axis ($F_{x_{wind}}$, aligned with the airspeed vector) yields

$$\sum F_{x_{wind}} = T\cos\alpha - D - W\sin\gamma. \tag{1}$$

The rate of change of altitude ("rate of climb"), $\dot{h}$, is related to the flight path angle and the velocity via

$$\sin\gamma = \dot{h}/V. \tag{2}$$

In steady flight, the forces are balanced. By setting Eq. (1) equal to zero and substituting in Eq. (2), the thrust is

$$T = \left[\left(\dot{h}W/V\right) + D\right]/\cos\alpha. \tag{3}$$

Summing the forces along the wind z-axis ($F_{z_{wind}}$), setting to zero for steady flight, and solving for lift yields

$$L = W\cos\gamma - T\sin\alpha. \tag{4}$$

If D is defined as the drag of the aircraft in the absence of any power-on effects, then T is the installed thrust (meaning the isolated thrust of the propeller modified by any cooling, scrubbing, blockage, lift-induced, or any other propulsion-airframe interaction). The drag force can be estimated from the drag polar developed using the power-off glide maneuver campaign described in our previous paper [5]. Lift and drag are nondimensionalized in coefficient form as

$$C_L = L/qS \tag{5}$$

$$C_D = D/qS \tag{6}$$

where C_L is the lift coefficient, C_D is the drag coefficient, q is the dynamic pressure, and S is the reference area. The reference area for Mod I and II is 14.76 m^2, and for Mod III/IV, it is 6.19 m^2 [1]. The power-off drag coefficient is

$$C_D = K_0 + K_1 C_L + K_2 C_L^2 \tag{7}$$

where K_0, K_1, and K_2 are polynomial coefficients computed per the previous paper [5]. From these relations, thrust, lift, and drag can be determined iteratively by guessing an initial value for lift (generally equal to weight), resolving power-off drag via Eq. (7) and Eq. (6), calculating installed thrust from Eq. (3), and then re-computing lift from Eq. (4) until the values for lift converge. In practice, Eqs. (3) and (4) typically use the small angle approximation for α and γ, in which case $\cos\alpha \to 1$, $\cos\gamma \to 1$, and $\sin\alpha \to 0$, and no iteration is then required to get lift, power-off drag, and installed thrust. However, as the X-57 project intended to directly measure angle of attack and the aircraft pitch angle, both forms (with and without the small angle approximation) are considered in this paper.

B. Gross Thrust Estimation

The cruise propeller selected for X-57 Mods II, III, and IV was the MT-Propeller MTV-7-152/64; a 1.52 m diameter, three-bladed propeller with an electrically actuated hub that operates in both a fixed pitch and constant speed mode [9]. Nominal X-57 operations were to be conducted with the cruise propeller in a control mode that emulated a constant-speed propeller. The manufacturer provided the X-57 team with proprietary performance data suitable to estimate gross thrust for a given flight condition. This was provided as a table of propeller efficiencies indexed to propeller power coefficients and advance ratios. These quantities are defined as

$$\eta_p = \frac{TV}{P} = \frac{C_T}{C_P} J \tag{8}$$

$$C_P = P/\rho n^3 D_p^5 \tag{9}$$

$$J = V/nD_p \tag{10}$$

where η_p is the propeller efficiency, T is the propeller thrust, V is the true airspeed, P is the shaft power, C_T is the thrust coefficient, C_P is the power coefficient defined by Eq. (9), J is the advance ratio defined by Eq. (10), D_p is the diameter of the propeller, ρ is the freestream density of air for the given flight condition, and n is the propeller speed.

The shaft power and speed are estimated from the electric propulsion system instrumentation in the X-57, and the air density and airspeed are derived from air data instrumentation. This provides the means to resolve Eqs. (9) and (10), which can be used to resolve the propeller efficiency from the manufacturer data. This efficiency estimate enables Eq. (8) to be rearranged to determine thrust. In this case, the efficiency table from the manufacturer is for an isolated propeller free of other installation losses and is gross thrust. The difference between the gross thrust and the installed thrust from Eq. (3) represents the installation effect for the flight condition under test, one of the key research objectives of the X-57 power-on test points.

C. Error Estimation

The installed thrust estimate in Eq. (3) and the gross thrust estimate determined from Eq. (8) are based on several in-flight measurements and a model of power-off aircraft drag, all of which are subject to errors. These include errors in the measurement of parameters derived from aircraft state data, errors in weight estimates, errors in the power-off drag model derived from Ref. [5], and non-ideal conditions such as turbulence that challenge the steady flight assumption. These error sources are described below.

1. Aircraft State Data Measurement

The X-57 incorporated a dedicated instrumentation system on board the aircraft to record and transmit aircraft state information from air, inertial, and satellite-derived measurements. These time-tagged measurements were used to estimate aircraft state, including altitude, airspeed, angle of attack, pitch angle, and flight path angle. The errors associated with these estimates could impact the precision of the installed thrust estimate.

The rate of altitude change, $\dot{h}$, would be inferred by measuring a change in altitude, Δh, over an elapsed time, Δt, in which the aircraft is in a steady flight condition (i.e., not accelerating). Thus, the error in $\dot{h}$ would be related to the error associated with the initial and final altitude estimate used to develop Δh as well as the timing error associated with Δt. The timing system had very small errors (generally << 0.1 s) as compared to the altitude error, so the errors in $\dot{h}$ would be dominated by error in the altitude measurement. The error in the static pressure estimate was driven by requirements for altitude measurement. Appendix E of Part 43 of Title 14 of the Code of Federal Regulations provides requirements for altimeter errors [10]. This material indicates that an altimeter shall have an error of no more than ±60 ft at an altitude of 8,000 ft MSL, which are assumed in this paper to occur at a 95% confidence level. The project calibration goals for airspeed were ±1 KTAS at a 95% confidence at the conditions associated with the target cruise condition of 150 KTAS and 8,000 ft MSL.

The estimate of α had a calibration goal of ±0.25° at a 95% confidence level (refined since the ±0.5° value used previously [5]). The measurement of γ was inferred by the difference in θ and α per Fig. 2, meaning the total error would be related to measurements. In the previous study, the error in θ was estimated as ±0.15° at a 95% confidence level [5]. This is simplified in this paper assuming both errors are random; hence the error in γ for this paper is assumed to be the Pythagorean sum of the combined errors in θ and α, or ±0.29°. Rather than track error in γ as a separate term, for simplicity, this paper uses the error in α (±0.25° at a 95% confidence level) as a surrogate for the error in γ, given that the error in α is the dominant term for error in γ.

2. Aircraft Weight

Aircraft weight is an important measurement for interpretation of flight data. The X-57 was uncommon among typical powered aircraft in that it did not burn fuel during flight. Instead, it was powered by batteries, which do not change weight during nominal operations. Therefore, the only appreciable errors that would exist in the aircraft weight would be associated with the method used to estimate the aircraft weight prior to each mission. The aircraft would be carefully weighed in the mission configuration as part of the development process but weighing prior to each flight was not planned. As such, errors in the weight could come from errors associated with the estimated versus actual weight of the flight crew (including any equipment used by the flight crew) and from small changes in weight due to swapping of installed equipment without performing a full re-weighing of the aircraft. In the previous paper, estimates were made with up to a ±25-pound weight error at the 68% confidence level (equal to one standard deviation of a normal distribution, σ) [5], which is continued in this paper.

3. Power-Off Drag

A key element of the estimation of installed thrust is the estimation of power-off drag for the given flight condition. The drag model given by Eqs. (6) and (7) is discussed at length in Ref. [5], which includes two methods for estimation of drag from a power-off flight maneuver. The so-called "method 1" approach is similar to the time-averaged approach discussed for installed thrust estimation using Eq. (3), and it was used to develop the experimental design of six test points recommended in Ref. [5] for the generation of the parameters for the power-off drag coefficient in Eq. (7). Overall, the power-off maneuvers were shown to likely result in errors of less than 5% per maneuver, resulting in a mean model representation error of 2.3% with a standard deviation of 1.5%.

4. Propulsion System Data

The gross thrust estimates relied on data from the propulsion system – namely, motor mechanical ("shaft") power and propeller speed. The X-57 cruise motor was directly connected to the propeller without a gearbox, so the propeller and motor speeds were identical. The X-57 used three independent sources of motor speed because this was such a crucial control parameter, and the motor speeds were generally found to have an error of much less than one revolution per minute (RPM). The motor shaft power was estimated as the product of the motor shaft torque estimate, Q, and the motor angular velocity derived from the shaft speed, n. A detailed motor performance map was planned for the project to better characterize error in the mechanical torque estimates from the motor controller, but it was never completed. However, preliminary dynamometer tests indicated that motor torque was generally within 1.0 Nm of the motor controller-generated torque estimate at typical flight torque settings (100-255 Nm) and well within 2.0 Nm. For this paper, we considered the 95% confidence interval on the torque estimate to be 2.0 Nm and did not consider error in the motor speed estimate due to its very low value.

5. Error Summary

A summary of the errors evaluated in this paper are given in Table 1. In all cases, the error was assumed to be normally distributed. For example, if a 95% confidence interval was specified, the standard deviation of the error was the specified error value divided by 1.96. Note that the airspeed calibration error goal provided in Section III.C was expressed as true airspeed around the cruise condition; this is corrected in Table 1 to equivalent airspeed to be applicable to the other X-57 test points. Errors in the measurement of the elapsed time for the maneuver and the motor shaft speed were not considered.

Table 1 Summary of error distributions for X-57 power-on maneuvers

Parameter	Symbol	Mean Error	Standard Deviation	Units
Angle of Attack	α	0.0	0.1276	degrees
Airspeed	V	0.0	0.4524	knots equivalent airspeed
Aircraft Weight	W	0.0	25.0	pounds-force
Altitude	h	0.0	30.61	feet mean sea level
Aircraft Drag	D	2.3%	1.5%	-
Motor & Propeller Torque	Q	0.0	1.020	newton-meter

IV. Analysis Approach

The power-on test points were established by the X-57 project to estimate the propulsion installation effects across a variety of expected flight conditions. These conditions are summarized in Table 2 for the Mod II configuration. Similar conditions were planned for the Mod III configuration to evaluate the changes in propulsion installation effects between Mod II and Mod III, but these were never finalized prior to the end of the project. As such, only the Mod II test points are considered in this paper.

Table 2 X-57 Mod II power-on test points

Test Point	Identifier	V, KEAS	Q, Nm	N, RPM	h, ft	W, lbf
Climb Speed 1	CL1	85	255	2250	5000	3000
Climb Speed 2	CL2	90	255	2250	6000	3000
Climb Speed 3	CL3	100	255	2250	7000	3000
Cruise Speed 1	CR1	85	123	2250	6000	3000
Cruise Speed 2	CR2	100	153	2250	6000	3000
Cruise Speed 3	CR3	110	179	2250	6000	3000
Cruise Speed 4	CR4	110	222	1800	6000	3000
Cruise Speed 5	CR5	110	201	2000	6000	3000
Cruise Speed 6	CR6	110	159	2500	6000	3000
Cruise Speed 7	CR7	120	217	2250	8000	3000
Max Continuous Power Cruise	VH1	128	255	2250	8000	3000
Project Cruise Speed Target	VC1	133	255	2550	8000	3000
Peak Power Cruise	VH2	136	255	2700	8000	3000

The power-on test maneuvers included climb and cruise test points. The climb points were intended to result in a net change in altitude during the maneuver, and the cruise points were intended to produce no net change in altitude during the maneuver. The simulated performance for each of these test points was developed by establishing the installed and gross thrust from the equations in the previous section using data from the X-57 Mod II performance models (aerodynamic, propulsion, and flight dynamics) described in a previous paper [11]. In Table 2, the power settings (motor torque and speed) for the cruise points reflect the expected settings for zero net change in altitude per the referenced performance models in still air and in the X-57 project Standard Day Reference Atmosphere [12], which is essentially identical to the 1976 U.S Standard Reference Atmosphere [3].

The impact of the error terms on the installed and gross thrust estimates associated with each maneuver was established by propagating the error terms from Table 1 using the X-57 Mod II performance models. In the case of the cruise points, no attempt was made to adjust the power settings to maintain zero net change in altitude; rather, any propagation of error terms that led to a change in altitude for the given power setting (with the error estimates applied, as appropriate) was used to modify the estimate of $\dot{h}$ in Eq. (3).

A. Pseudorandom Error Propagation

The impact of the errors from Table 1 on installed and gross thrust estimates for each of the test points was evaluated using a Monte Carlo simulation technique, in which repeated samples were obtained from a pseudorandom number generator emulating the normal distribution. This information was used to quantify the expected error in the installed and gross thrust estimates for each test point, which helped to inform the number of repeated test points of each type (or if repeated points were even required).

Each of the parameters from Table 1 was assigned to an independent pseudorandom sample that was scaled by the parameter's associated mean and standard deviation. MATLAB's® `randn` function[††] [13] was used to generate the sample for each experiment. All experiments were bounded within three standard deviations from the mean to avoid significant outliers (any sample beyond three standard deviations was set to three standard deviations), and the seed value for each pseudorandom sample was specified (albeit varied throughout each trial in the experimental design) to ensure repeatability. Each experimental design contained 50 trials, and each trial generated a unique pseudorandom sample for each of the error parameters. Each of these 50 trials was repeated for the 13 test points in Table 2.

The generation of error estimates for C_D in Eqs. (6) and (7) involved two sets of pseudorandom samples because a mean error was specified in Table 1 but the sign of the mean error was not. A first pseudorandom sample was used to generate the sign for the mean error, and a second pseudorandom sample was used to generate the value for the

[††] MATLAB® R2020b was used for the analyses described in this paper.

deviation of the error from the mean (which could be positive or negative). The two values were summed to get a relative error in the drag estimate.

The generation of error estimates for $\dot{h}$ in Eq. (3) followed the approach expected to be used for the flight experiments – the estimates were first made for Δh that were then divided by an elapsed time Δt. The estimate of Δh was assumed to come from two independent altitude measurements at the beginning and end of the maneuver, so the error in Δh was scaled to the standard deviation from Table 1 by $1/\sqrt{2}$. This is a pessimistic estimate because the altimeter errors may contain a bias component that would be eliminated in the difference of two nearby altitudes used to generate Δh. As noted earlier, the error in the Δt measurement was considered negligible. However, the time period used for each maneuver was an important parameter and was treated as an independent variable. Each of the 50 trials was repeated for a Δt of 10, 20, 30, 40, 50, and 60 seconds. The prior work on power-off glide estimation [5] found acceptable experimental errors for each data point could be found for Δt in the glides of 30 seconds.

B. Error Sensitivity Analysis

An error sensitivity analysis was conducted to identify which of the error sources would have the most impact on the uncertainty in the measurements and to determine if there were interactions between the error parameters associated with estimates for installed or gross thrust. This information was used to identify where refinements in instrumentation or experimental procedures could be used to reduce error if necessary.

A two-level full-factorial experimental design was established for the six factors in Table 1, resulting in an experimental design with 64 trials. Each factor level was considered either at one standard deviation above the mean or one standard deviation below the mean. The only exception was related to the error in the aircraft drag coefficient because it included both a mean and a standard deviation, the low factor level for aircraft drag error was considered at the negative mean minus one standard deviation, and the high factor level was considered at the positive mean plus one standard deviation. These trials were only considered for a single Δt that was selected after inspection of the error propagation experiments. The trials were repeated for each of the 13 test points in Table 2.

V. Results of Computational Experiments

The results of the computational experiments were scrutinized to determine the impact of elapsed time during each experiment, the impact of error propagation on gross thrust estimation, the impact of error propagation for individual test points for a selected elapsed time, and the sensitivity of the installed thrust estimates to the individual measurement errors. The subsections below describe the results of these investigations. In all cases, "truth" data was derived from the installed and gross thrust estimates based on the X-57 Mod II performance model [11] assuming zero error at the conditions specified in Table 2. The results that follow provide installed thrust and gross thrust elements relative to the "true" values from the same models without error rather than the raw values themselves. This is to protect the privileged information provided by the airframe and propeller vendors that was used to generate these dimensioned estimates.

A. Impact of Elapsed Time on Error Propagation for Installed Thrust Estimation

The pseudorandom error propagation experiments included variation of elapsed time per trial to help determine the appropriate amount of time to gather data for an individual flight maneuver. As shown previously for the power-off glide evaluation, longer time periods generally reduce the impact of error propagation for timed maneuvers [5]. However, longer time periods reduce the number of test points that can be evaluated for a given flight, which is particularly challenging for the X-57 given its limited energy storage capacity and therefore limited flight time.

Data were extracted from the computational experiments for the relative installed thrust estimate from Eq. (3) and normalized to the "true" installed thrust for each pseudorandom trial for each test point. The distributions of this relative installed thrust estimate are shown as box plots in Figs. 3 and 4. In Fig. 4, the small angle assumption for angle of attack is used. Both approaches are described at the end of Section III.A. Note that each box plot represents a frequency distribution containing 650 data points (50 pseudorandom trials for each of the 13 test points).

Visual inspection of the results with and without the small angle assumption for angle of attack indicates no appreciable difference between the distribution of the results for each of the two techniques. The numerical results of the statistics of the resulting distributions are given for the iterative approach in Table 3 and for the small angle approach in Table 4. Scrutiny of these results indicates that estimates for installed thrust using the small angle assumption are generally well within 0.5%, and typically 0.1%, of the installed thrust estimates using the iterative approach.

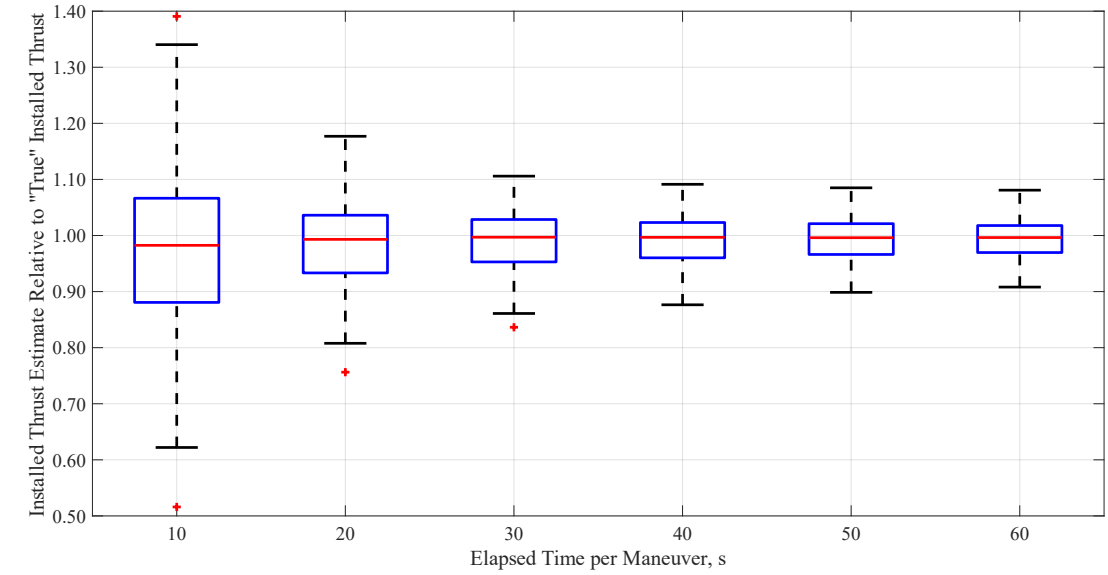

Fig. 3 Distribution of relative installed thrust estimate versus elapsed time per maneuver across all maneuvers using the iterative method for angle of attack.

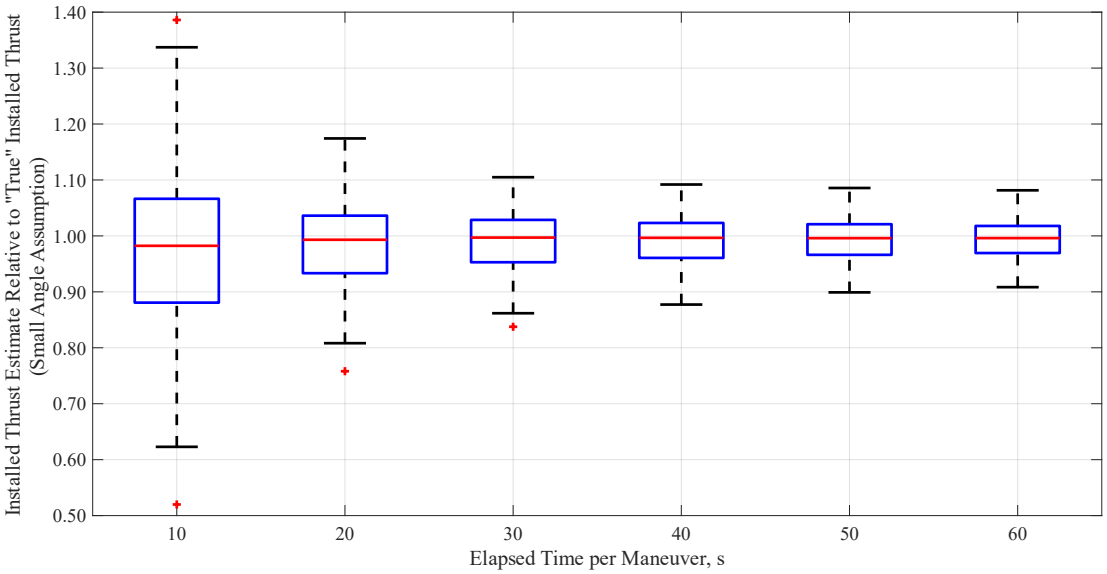

Fig. 4 Distribution of relative installed thrust estimate versus elapsed time per maneuver across all maneuvers using the small angle assumption for angle of attack.

The impact of the elapsed time per maneuver shows a strong yet diminishing effect as Δt increases. The middle quartile bounds for the upper and lower estimates from the mean improve only 0.54% and 0.04%, respectively, for Δt values of 60 s as compared to 40 s. The upper and lower adjacent bounds improve by about 1.0% each for Δt values of 60 s as compared to 40 s. This is similar to the conclusion from evaluation of the power-off glide maneuvers in the previous paper [5] that sufficient error reduction could occur over maneuver time periods of 30 s. Elapsed times as low as 10 s may be tolerable if repeated test points could be made at the same condition, but for this paper, 40 s was selected as the elapsed maneuver time for subsequent analysis.

Table 3 Distribution statistics for relative installed thrust estimate versus elapsed time per maneuver across all maneuvers using the iterative method for angle of attack

Δt, s	10	20	30	40	50	60
Upper Adjacent	1.3403	1.1769	1.1059	1.0913	1.0850	1.0808
75th Percentile	1.0664	1.0362	1.0285	1.0232	1.0211	1.0178
Median	0.9825	0.9931	0.9970	0.9967	0.9961	0.9963
25th Percentile	0.8807	0.9333	0.9529	0.9602	0.9662	0.9696
Lower Adjacent	0.6220	0.8078	0.8610	0.8765	0.8986	0.9081
Outliers	2	1	1	0	0	0

Table 4 Distribution statistics for relative installed thrust estimate versus elapsed time per maneuver across all maneuvers using the small angle assumption for angle of attack

Δt, s	10	20	30	40	50	60
Upper Adjacent	1.3372	1.1742	1.1049	1.0919	1.0856	1.0815
75th Percentile	1.0663	1.0362	1.0286	1.0232	1.0209	1.0178
Median	0.9823	0.9931	0.9970	0.9966	0.9960	0.9961
25th Percentile	0.8807	0.9333	0.9529	0.9607	0.9615	0.9694
Lower Adjacent	0.6229	0.8082	0.8617	0.8773	0.8991	0.9084
Outliers	2	1	1	0	0	0

B. Impact of Error Propagation on Gross Thrust Estimation

The pseudorandom error propagation experiments included variation of parameters related to the estimation of gross thrust. The resulting distribution of relative gross thrust for each of the 50 pseudorandom trials aggregated over all the 13 test points is shown in Fig. 5. The distribution statistics show that relative gross thrust was expected to be between 0.9953 and 1.0044 at the 25th and 75th percentile, and between a lower adjacent and upper adjacent of 0.9822 and 1.0178. Errors within the manufacturer data used to estimate the gross thrust were not available and therefore not estimated nor included in this analysis.

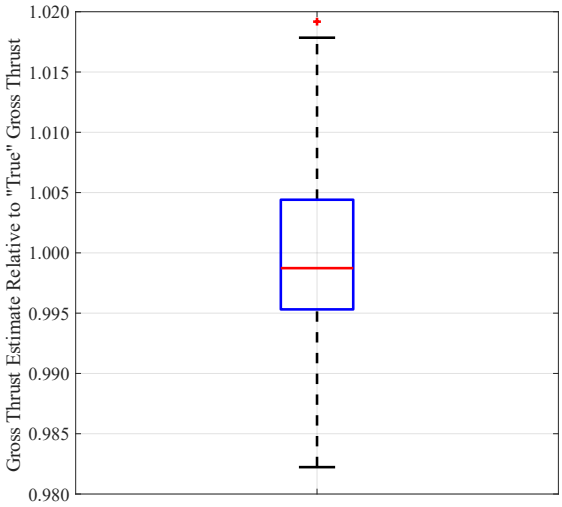

Fig. 5 Distribution of relative gross thrust across all maneuvers.

C. Impact of Error Propagation on Installed Thrust Estimation for Individual Test Points

The error propagation results discussed in Section V.A and V.B considered the installed and gross thrust aggregated across all 13 of the test points from Table 2. As seen from Fig. 5, the variation in relative gross thrust for the individual maneuvers is likely quite small, but the ranges seen in Figs. 3 and 4 indicate larger variation that may be more significant across the test points. The distribution of relative installed thrust estimates is shown in Fig. 6 for propagation of the 50 pseudorandom error samples on each of the 13 test points for a maneuver time of 40 s.

Close inspection of Fig. 6 reveals that the cruise test points exhibit larger error distributions than the climb test points. This is likely because the dimensional installed thrust of the climb test points is higher than the cruise test points; many of the cruise test points are at lower power settings than the climb test points. All the climb test points are at the same power setting as the VH1 cruise test point per Table 2. The VC1 and VH2 cruise test points are both at higher power settings than the climb test points, but also higher velocities, which may contribute to the larger error trends as compared to the climb test points. The largest error is observed in the CR1 cruise test point, which happens to be at the lowest power setting and therefore the lowest installed thrust estimate. Excluding the CR1 cruise test point, the upper and lower quartiles indicate that the relative installed thrust estimate for each maneuver will be within 5% of the "true" value. This is encouraging if a model of installed thrust difference compared to the gross thrust could be created from flight data, much as a known model for vehicle drag (a drag polar) was developed in the previous paper [5] that enabled aggregate model error reduction vs individual error in the test points (the prior work indicated individual test points had error propagation estimates of around 5%, but the overall model mean error dropped to 2.3% when reduced to a drag polar). Additionally, repeated test points can reduce random error, and the data from Fig. 6 could be used to target repeated test points. In particular, repeated climb points would have been necessary to get on condition for other test objectives and could have served as a data source for repeated measurements.

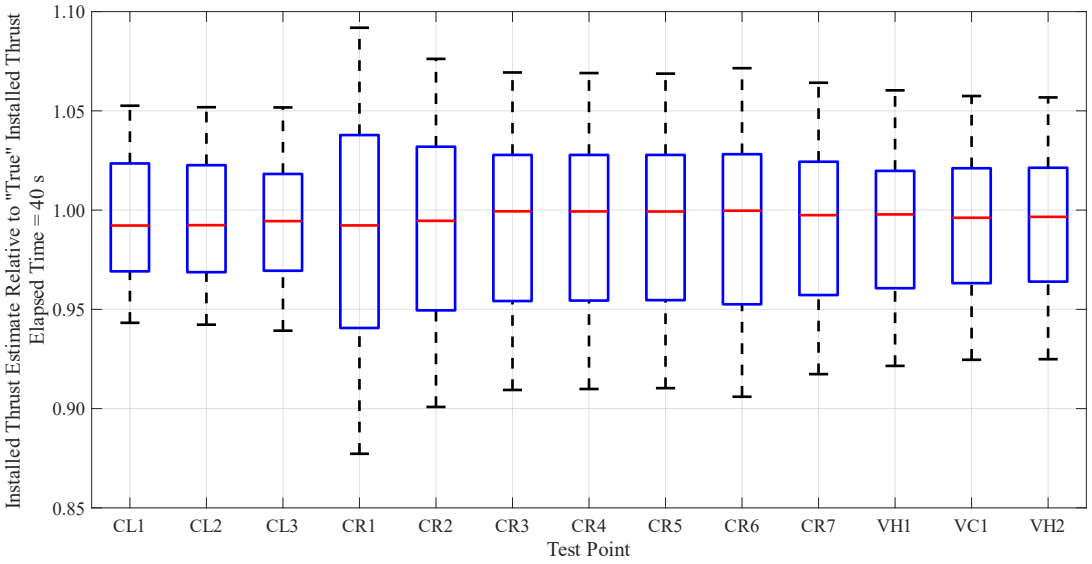

Fig. 6 Distribution of relative installed thrust estimate for each maneuver for an elapsed time of 40 s.

D. Sensitivity of Installed Thrust and Gross Thrust to Individual Errors

The results of the pseudorandom error propagation experiments shown thus far consider the impacts of the aggregate propagation of error on the installed and gross thrust estimates. A sensitivity analysis was performed using a two-level, full factorial design of experiments on the six error factors as discussed in Section IV.B. This included analysis of the main effects of each individual parameter from Table 1. The main effects of the individual error factors on each of the 13 experiments is shown in Fig. 7 for the relative installed and gross thrust estimates. The main effects are also shown in Table 5 for the relative installed thrust and Table 6 for the relative gross thrust.

The variation among the test points for the relative gross thrust (right side of Fig. 7 and Table 6) is generally lower than for the relative installed thrust and is isolated to torque, airspeed, and altitude. Not surprisingly, the test points with lower torque settings show higher error impacts because error was specified as a dimensional estimate and not relative. The variations in relative gross thrust for airspeed and altitude do not seem to follow any macro trend, and any variations are likely dominated by individual changes in the pseudorandom samples. The dominant error terms include error in the torque estimate and airspeed, followed by a very minor impact from error in the altitude measurement. The latter is likely due to the impact of altitude error on the estimation of atmospheric parameters (e.g., air density) on the models used to estimate gross thrust.

The main error effects show variation but generally similar trends for each of the experiments. The most impactful error terms for relative installed thrust are the estimate of the aircraft drag and altitude, followed by weight and airspeed. Error in angle of attack has almost no impact, and error in torque has no impact on relative installed thrust (as expected, given the derivation in Section III). The variation among each of the test points is different for many of

the individual error terms for relative installed thrust (left side of Fig. 7 and in Table 5). The impact of error in drag lessens at the combination of lower airspeeds and higher powers seen in the climb points, likely because the excess thrust at these lower drag (lower airspeed) conditions is being converted into rate of climb. The impact of altitude measurement errors on relative installed thrust increases for the cruise test points that are the combination of lower airspeed (lower drag) and lower power setting (lower thrust) conditions. This could provide a rationale to target more precise altitude measurements for these maneuvers to reduce the expected error in the altitude measurement. The impact of weight errors on relative installed thrust estimates decreases as the airspeed of the test points increase, which is likely due to the impact that weight has on the lift coefficient seen in Eq. (5) for higher airspeeds (and therefore higher dynamic pressures). Higher speed lowers the lift coefficient and its impact on the vehicle drag. Curiously, for relative installed thrust the main effect of airspeed error reverses its trend (from a negative to positive net main effect) for the lowest-speed climb points as compared to the other test points. The reason for this is not explored further in this paper, but this behavior is noted as an observation for future investigation.

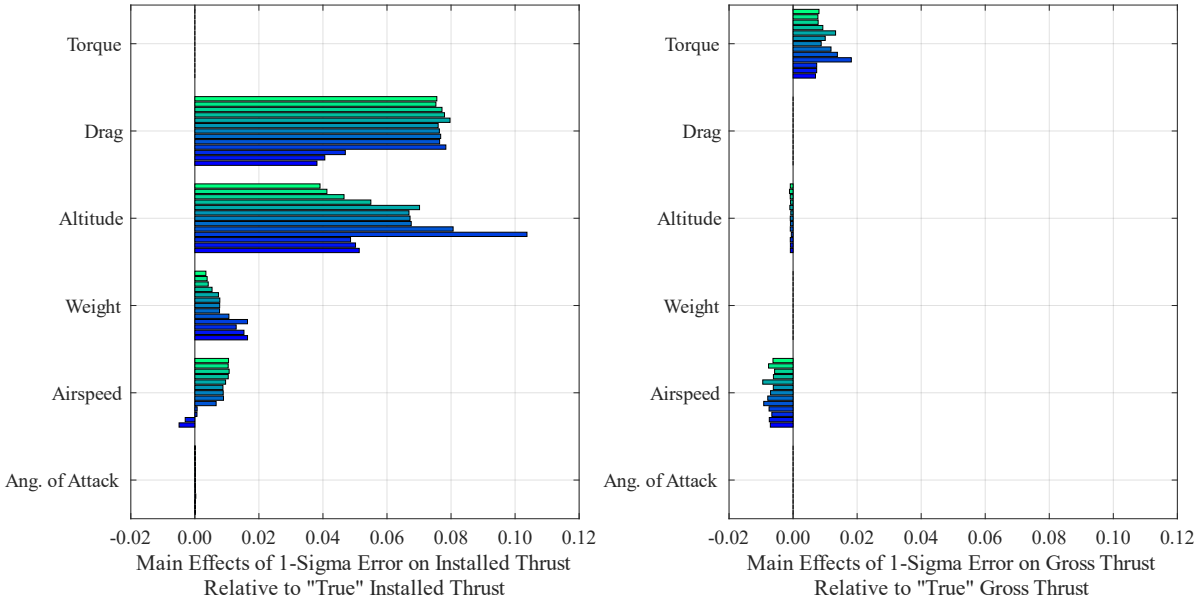

Fig. 7 Main effects of positive and negative variation of mean plus one standard deviation of error on relative installed thrust (left) and relative gross thrust (right). Test point #1 is the lowest (darkest blue bar) and test point #13 is the highest (lightest green bar) in each parameter grouping.

Table 5 Main effects of positive and negative variation of mean plus one standard deviation of error on relative installed thrust

Test point	Angle of Attack	Airspeed	Weight	Altitude	Drag	Torque
CL1	0.00014	-0.00493	0.01645	0.05133	0.03813	0.00000
CL2	0.00013	-0.00301	0.01534	0.05017	0.04059	0.00000
CL3	0.00011	0.00067	0.01291	0.04862	0.04699	0.00000
CR1	0.00029	0.00072	0.01644	0.10372	0.07838	0.00000
CR2	0.00019	0.00664	0.01063	0.08065	0.07644	0.00000
CR3	0.00015	0.00895	0.00771	0.06757	0.07677	0.00000
CR4	0.00015	0.00886	0.00775	0.06720	0.07636	0.00000
CR5	0.00015	0.00877	0.00780	0.06687	0.07598	0.00000
CR6	0.00015	0.00960	0.00737	0.07017	0.07969	0.00000
CR7	0.00012	0.01043	0.00537	0.05496	0.07796	0.00000
VH1	0.00010	0.01071	0.00418	0.04658	0.07718	0.00000
VC1	0.00008	0.01041	0.00384	0.04124	0.07528	0.00000
VH2	0.00008	0.01052	0.00345	0.03909	0.07557	0.00000

Table 6 Main effects of positive and negative variation of mean plus one standard deviation of error on relative gross thrust

Test point	Angle of Attack	Airspeed	Weight	Altitude	Drag	Torque
CL1	0.00000	-0.00710	0.00000	-0.00085	0.00000	0.00700
CL2	0.00000	-0.00743	0.00000	-0.00084	0.00000	0.00737
CL3	0.00000	-0.00663	0.00000	-0.00088	0.00000	0.00738
CR1	0.00000	-0.00750	0.00000	-0.00056	0.00000	0.01819
CR2	0.00000	-0.00917	0.00000	-0.00088	0.00000	0.01384
CR3	0.00000	-0.00791	0.00000	-0.00083	0.00000	0.01184
CR4	0.00000	-0.00703	0.00000	-0.00088	0.00000	0.00878
CR5	0.00000	-0.00617	0.00000	-0.00072	0.00000	0.01004
CR6	0.00000	-0.00947	0.00000	-0.00101	0.00000	0.01327
CR7	0.00000	-0.00614	0.00000	-0.00080	0.00000	0.00929
VH1	0.00000	-0.00577	0.00000	-0.00089	0.00000	0.00783
VC1	0.00000	-0.00766	0.00000	-0.00112	0.00000	0.00775
VH2	0.00000	-0.00628	0.00000	-0.00087	0.00000	0.00809

VI. Summary and Concluding Remarks

The determination of installed thrust characteristics and the differences between gross and installed thrust are important characteristics for aircraft performance. NASA's X-57 project sought to explore two of these interactions – the changes in installation effects for electrified propulsion with the X-57 Mod II configuration and the addition of wingtip-mounted propellers to capture an installation benefit between the propeller rotation and the wingtip vortex in the X-57 Mod III/IV configuration. The X-57 flight test plan included several power-off and power-on maneuvers to determine the drag and installed thrust characteristics of the different X-57 Mods. A previous paper ("Part 1") discussed two methods for determination of power-off drag from glide maneuvers and showed how, in the presence of expected measurement errors and variations in flight test techniques, the test program could use three power-off test points each repeated once (for six experiments) to generate a drag model with a mean error of 2.3% and a standard deviation of 1.5% when using existing computational models as a "truth" source in simulation [5]. This paper ("Part 2") identified the procedures and possible error sources for the power-on maneuvers used in conjunction with the power-off drag models to estimate installed thrust, as well as the method to estimate the gross thrust to help determine the impact of propulsion system integration on X-57 performance in Mods II and III/IV.

A. Error Propagation Impact on Thrust Estimates

A total of 13 test points identified by the X-57 project personnel were of interest for further examination of the installation effects on the propulsive thrust. Unlike the power-off drag predictions, there were no well-established models of installed thrust losses that could be used to guide the selection of test points. Rather, the intent was to propagate the error terms through the proposed measurement and data reduction techniques to determine the amount of error in the estimates of installed thrust and gross thrust for each of the test points.

The error was propagated to the installed and gross thrust measurements via established computational models and pseudorandom sampling of a normal probability distribution of error terms associated with aircraft instrumentation or test technique. These samples were repeated for six different simulated maneuver durations to determine the impact of maneuver duration on the error in the installed thrust estimate for each maneuver. The resulting distributions showed that, when aggregated across all 13 test points, an elapsed maneuver time of 40 s was expected to yield an installed thrust estimate between -3.9% and +2.3% of the "true" value at the 25th and 75th percentile, respectively. This 40 s maneuver time was slightly longer than the 30 s period used for the power-off glide maneuvers in the previous paper. Additionally, comparison of a technique that accounted for angle of attack with one that discounted it due to the small angle assumption indicated a difference of less than 0.5% (and in many cases less than 0.1%) for the installed thrust estimate when using the small angle assumption.

The impact of error propagation on gross thrust estimates was much smaller, though no error estimates were available from the manufacturer data for the propeller. Obviously, if the error in the manufacturer estimates can be quantified, the error estimates for gross thrust can be improved. Assuming perfect manufacturer data, the other error sources identified in this paper contribute to 0.5% error in the gross thrust estimate at a 50% confidence (25th to 75th percentile).

Some individual test points were found to be more sensitive to error than others. Test points at lower power settings and lower speeds exhibited higher installed thrust error estimates. These test points would benefit from repeated passes in the flight test plan to reduce experimental error to within 5%.

B. Sensitivity of Thrust Estimates to Error Sources

The error sources identified in this paper for the X-57 flight maneuvers were found to have different contributions to the propagated error in the installed and gross thrust estimates. The errors in the aircraft drag and altitude measurements were found to be the dominant sources of error for installed thrust estimation, followed by weight and airspeed error. The error in the gross thrust measurement was dominated by errors in the motor torque and airspeed measurements. Neither installed thrust nor gross thrust exhibited any appreciable error associated with variations in the angle of attack measurement.

C. Paths for Improvement

The error propagation approach used in this paper assumed errors in the measurement of altitude were random and independent. However, the specification used to certify altimeters indicates that bias error may be present. The method used to estimate installed thrust relied on measuring the change in altitude during the maneuver. The error in that measurement that may be much smaller if the altitude error was dominated by bias rather than random error.

Errors in the drag estimates were one of the major contributors to error in the installed thrust estimation. The authors' previous work on power-off glide points included a maneuver suite with nine experiments that reduced the mean error for the drag estimate to less than 2% and the standard deviation of error to about 1% (as compared to 2.3% and 1.5% for the six-experiment model that was used in this paper). The test program for X-57 was able to gather three power-off test points per flight (given the high rate of descent seen for some of these test points), so this would require one more flight.

This paper did not identify an installation change model for the propulsion system, but rather the method used to estimate the installed and gross thrust. An installation model, like a drag polar, would provide a reference frame where multiple different test points (rather than just measurements repeated at the same test point) could help reduce aggregate error. Additionally, test campaigns could be developed that emphasized only certain areas of the flight envelope. If test points are at a premium, more targeted selection of test points or repeated points may be necessary.

Finally, the prior paper noted an approach ("method 2") that directly solved for drag, lift, and sideforce terms from high-rate air and acceleration data throughout the power-off glide maneuver rather than over an elapsed time period [5]. This method provided generally accurate estimates, but the extremes of the propagated error were found to be too high for this method to be used as the primary source of the lift, drag, and sideforce terms. However, if the data were found to be reliable, the use of "method 2" could provide a much more precise power-off drag estimate to reduce the error for the calculations in this document.

Acknowledgments

This work was funded by the Flight Demonstrations and Capabilities Project within the Integrated Aviation Systems Program of NASA's Aeronautics Research Mission Directorate. The authors thank NASA for their financial and technical support of this effort.

References

[1] Borer, N. K., Patterson, M. D., Viken, J. K., Moore, M. D., Clarke, S., Redifer, M., Christie, R., Stoll, A., Dubois, A, Bevirt, J., Gibson, A., Foster, T., Osterkamp, P., "Design and Performance of the NASA SCEPTOR Distributed Electric Propulsion Flight Demonstrator," AIAA Paper 2016-3920, June 2016 (doi: 10.2514/6.2016-3920). Publicly available at https://ntrs.nasa.gov/citations/20160010157, [retrieved 10 June 2024].

[2] Costruzioni Aeronautiche Tecnam S.r.l, "P2006T – Aircraft Flight Manual," Doc. No. 2006/044, 4th Ed., Italy, 2015.

[3] National Aeronautics and Space Administration, "U.S. Standard Atmosphere, 1976," NASA-TM-X-74335, October 1976.

[4] National Aeronautics and Space Administration, "Scalable Convergent Electric Propulsion Technology and Operations Research (SCEPTOR) Critical Design Review: Day 2 Package," November 2016. Publicly available at https://www.nasa.gov/sites/default/files/atoms/files/sceptor_cdr_day_2_package.pdf, [retrieved 10 June 2024].

[5] Borer, N. K., Cox, D. E., Wallace, R. D., "Flight Performance Maneuver Planning for NASA's X-57 "Maxwell" Flight Demonstrator – Part 1: Power-Off Glides," AIAA Paper 2019-2855, June 2019 (doi: 10.2514/6.2019-2855). Publicly available at https://ntrs.nasa.gov/citations/20190033419, [retrieved 10 June 2024].

[6] Mattingly, J. D., Heiser, W. H., Pratt, D. T., *Aircraft Engine Design, Second Edition*, American Institute of Aeronautics and Astronautics, Reston, Virginia, 2002.

[7] Veldhuis, L. L. M., *Propeller Wing Aerodynamic Interference*, Ph.D. Thesis, Delft University of Technology, June 2005.

[8] Miranda, L. R., Brennan, J. E., "Aerodynamic Effects of Wingtip-Mounted Propellers and Turbines," AIAA Paper 86-1802, 1986.
[9] U. S. Department of Transportation, Federal Aviation Administration, "Type Certificate Data Sheet P-20BO, MT-Propeller Company, Model MTV-7-( )," TCDS Number P20BO, Revision 2, March 2007.
[10] Title 14, Chapter I, Subchapter C, Part 43, Appendix E, "Altimeter System Test and Inspection," United States Code of Federal Regulations, Amendment 43-49, 81 FR 96700, December 2016.
[11] Wallace, R., Reynolds, J., Frederick, M., McMinn, D., Cox, D., Borer, N., "Development of the Mod II X-57 Piloted Simulator and Flying Qualities Predictions," AIAA Paper 2023-4034, June 2023 (doi: 10.2514/2023-4034). Publicly available at https://ntrs.nasa.gov/citations/20230004174, [retrieved 10 June 2024].
[12] Wilhite, J. M., Borer, N. K., Frederick, M. A., "Thermal Environments and Margin Guidelines for NASA's X-57 "Maxwell" Flight Demonstrator," AIAA Paper 2024-1475, January 2024 (doi: 10.2514/6.2024-1475). Publicly available at https://ntrs.nasa.gov/citations/20230017892, [retrieved 10 June 2024].
[13] MathWorks, "randn: Normally distributed random numbers," https://www.mathworks.com/help/matlab/ref/randn.html, [retrieved 5 June 2024].